Dynamics in thermoreversible polymer gels

H. B. Bohidar*

Chemistry Department, Purdue School of Science, Purdue University, Indianapolis Campus, IN 46202, USA

Polymer gels are a novel state of matter having both solid and liquid-like properties. Once cross-linked, the polymer chains lose their identity and become part of a large three-dimensional inter-connected cluster pervading through the entire volume. Such a system has both fluidity and elasticity. The associated osmotic elastic moduli characterize the gel strength and porosity of the gel. The dynamics of this is very revealing. Several relaxation modes are observed in these systems which are obtained through either dynamic structure factor or rheological measurements. This has been examined in detail for physical gels. A second problem is the transport of probe particles through the gel network. This is an anomalous diffusion process and necessitates the reformulation of the normal diffusion problem by invoking non-ergodicity concepts. This has direct bearing on transport of proteins through membranes which are close to cross-linked networks. We discuss the associated dynamics in detail.

MOSTLY flexible polymers exhibit unique physical features when the thermodynamic environment is altered. One of the several possible manifestations of this phenomenon is the gelation. Bio-polymeric gels are present in abundance in living organisms; in our body, the cornea, the vitreous, and the connective tissues are all gels. Gels serve as excellent surfaces of the internal tracts such as stomach, lungs, kidney basement, and blood vessels. Gels perform an important task here; these are permeable to mobile ions and water but impermeable to body waste. Thus gels prevent the toxic materials from entering the vital organs. Gels are known to mankind for long, though the salient features of gelation mechanisms have been revealed through intensive theoretical and experimental studies carried out in the last three decades.

What is a polymer gel and how does it differ from a branched polymer, network cluster or a grafted polymer? There are several ways to identify a true gel. Herman[1] defined a gel as: 'A coherent system of at least two components, which exhibits mechanical properties characteristic of a solid, where both the dispersed component and the dispersion medium extend throughout the whole system'. According to Ferry[2], 'it is a substantially diluted system which cannot exhibit steady state flow'. Kramer[3] extended Herman's definition to add that 'a gel state is one that has a finite modulus with a pronounced plateau extending to the time scales of seconds accompanied by a small loss modulus in this region'. An equilibrium shear modulus develops at the onset of gelation. Several alternative definitions exist. The polymerization of a monomer unit with functionality (number of binding sites) > 2 can in principle, give rise to a three-dimensional interconnected giant supra molecular structure in the solution phase (see Figure 1). However, such a structure does not always possess all the features of a gel. Normally, long-chain polymers are crosslinked chemically in the solvent medium to produce a chemical gel, which are rigid and can sustain significant amount of compressional and shear deformations. These are generally understood and described through percolation theory.

On the other hand, physical gels are formed and stabilized in the solvent mostly through secondary forces like hydrogen bonding, van der Waal's forces, hydrophobic interactions, etc[4]. Hence, these are fragile compared to chemical gels that are formed as a result of primary forces (covalent bonding). Thermoreversible

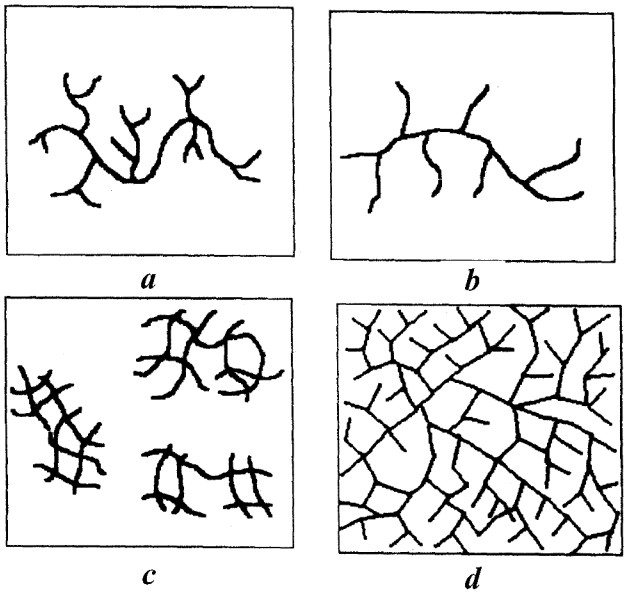

Figure 1. *a*, a branched polymer, *b*, a grafted polymer, *c*, a network cluster (microgel) and *d*, a gel state. Notice that in *d* all the chains are part of the same giant network that pervades through the whole volume unlike in *a*, *b* or *c*.

*On leave from School of Physical Sciences, Jawaharlal Nehru University, New Delhi, India.

gels are mostly physical gels. Examples are gelatin[5], poly(vinyl chloride), poly(acrylonitrile), polystyrene (atactic), poly(vinyl alcohol), agarose, carrageenans, benzohydroxamic acid, cellulose, and polysaccharides[6], etc. However, the common feature is the evolution of an infinitely large and connected network with a characteristic mesh size (also called correlation length). In the critical phase transition picture the correlation length ξ and the mass (M) of the infinite network diverge at the gelation point following the scaling

$$M \propto \{(T/T_g) - 1\}^{-\gamma}, \quad (1)$$

and

$$\xi \propto \{(T/T_g) - 1\}^{-\nu}, \quad (2)$$

where T_g is the gel transition temperature. For ferromagnets, liquid–gas phase transitions and binary fluid mixtures, the theoretical prediction for the exponents γ and ν are given by the 3-D Ising model, which predicts[7,8] $\gamma = 1.24$ and $\nu = 0.63$. The percolation theory rests mostly on the same theoretical frame work and the same concepts are applied to describe the gelation in chemically crosslinked gels (the exponents are different, for example[9] $\gamma = 1.8$). As has already been said, as the incipient gel phase is approached, the system develops an equilibrium modulus G_e that increases with crosslink density[10,11]. The viscosity of the system diverges at T_g and often this is accepted as the signature of gel phase (see Figure 2). A polymer of molecular weight M, dissolved in a solvent with concentration C has three distinct fractions. One fraction of polymers actually belongs to the network and contributes to the elasticity (w_m), another fraction belongs to the network but does not contribute to elasticity (w_f) (dangling ends) and a third fraction (w_s) is not part of the network. Obviously, $(w_s + w_f + w_m) = 1$. Consequently[10],

$$G_e = (CRT/M)\,[-(1 + w_s) \ln w_s - 2\,(1 - w_s)]. \quad (3)$$

Other terms have their usual meaning. This equation applies to monodisperse polymers with functionality = 4. Many chemical gels are known to follow these features. All gels are associated with characteristic mesh structures. This is sometimes modeled as a blob of radius ξ which has a size equivalent to correlation length. The mesh size is a physically measurable parameter and can be found from neutron, light or X-ray scattering measurements. The density fluctuations in gels give rise to scattering of light. These propagate like phonons in the gel medium and the equation of motion can be written as[12]

$$\rho \frac{\partial^2 u(x,t)}{\partial t^2} = E \frac{\partial^2 u}{\partial x^2} - f \frac{\partial u}{\partial t}. \quad (4)$$

The equation represents the displacement u of a point in the gel, the longitudinal elastic modulus is E and f is the translational frictional coefficient (between the network and water). This constitutes the propagation of an acoustic wave in a visco-elastic medium. In most gels, the left hand term (inertial force) is much smaller than elastic restoring force and frictional force and, hence can be neglected. Hence one has

$$\frac{\partial u}{\partial t} = \frac{E}{f} \frac{\partial^2 u}{\partial x^2}, \quad (5)$$

and this resembles a diffusion equation although the network is interconnected and physically quite different from a two component solute-solvent system. These modes are known as collective diffusion modes in gels. Corresponding collective diffusion coefficient D_c, relates to the visco-elastic parameters as

$$D_c = E/f. \quad (6)$$

Since osmotic pressure drives the diffusion process, it is customary to refer to E as E_{os}, called longitudinal osmotic modulus. We can further imagine that each mesh is an entity of its own and has a radius ξ (called a blob earlier). From ideal gas law, if we have n such entities (per unit volume) $E_{os} = nk_BT$ and from Stokes law $f = n6\pi\eta\xi$. This will give the D_c value as[13]

$$D_c = k_BT/6\pi\eta\xi. \quad (7)$$

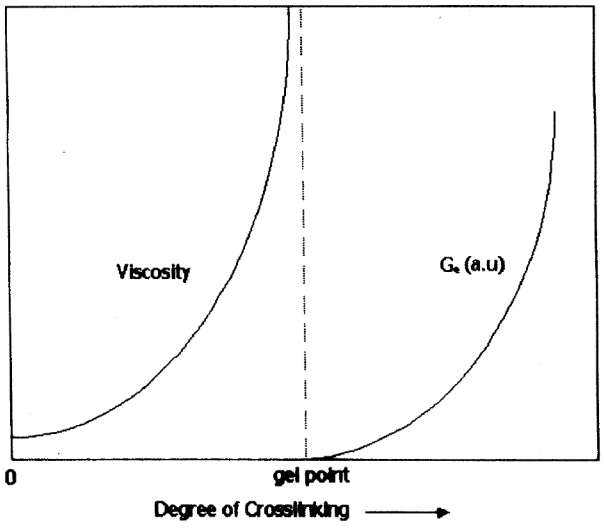

Figure 2. Divergence of viscosity is a signature of the incipient gel phase. Once the gel state is realized, the system develops an equilibrium modulus G_e as shown in this diagram. The solution state viscosity can grow 3 to 4 decades as the gel state is approached.

This is identical to Stoke–Einstein relation for a spherical particle of radius ξ diffusing in a solvent of viscosity η independently. We visualize each of these of radius ξ as a blob. The collective diffusion has been observed in many physical and chemical gels[6].

However, physical gels often cannot be described through percolation models because of difference in their structures. We will discuss the dynamical features of thermoreversible physical gels through gelatin which is denatured collagen and undergoes thermoreversible gelation in hydrogen-bond friendly environment, when the polypeptide concentration exceeds[5] $\approx 1\%$ (w/v). It is a biopolymer with a typical molecular weight of $\approx 10^5$ Da. Gelatin gels have been widely studied as thermoreversible gels where interconnected triple helices constitute the network which ultimately traps the solvent as hydration and interstitial water[14–17]. Interestingly, it is the only natural biopolymer that forms triple helices mostly through inter-helix hydrogen bonding.

It is also possible to produce a chemically cross-linked gelatin gel through usage of cross-linkers[18]. Though the kinetics of physical gelation of gelatin has been addressed in many in-depth investigations, what seems to be lacking is the adequate exploration of gelatin solutions where these molecules are chemically cross-linked. Chemically cross-linked gelatin is used in surgical absorbent powders, hectograph films, in pharmaceutical capsules, in tanning, etc. The common crosslinkers are metal salts, formaldehyde, glutaraldehyde, aldehyde sugars, di-substituted carbodiimides, ephichlorohydrin, etc[19]. Most of the discussion that follows is general and non-specific to any particular system but the data pertain to gelatin gels[5].

Experimental methods

The physical preparation method of gels differs from case to case and one can refer to literature for details[4–6]. But there are certain universal conditions. Normally, the polymer has a concentration above the overlap concentration C^* given by[20]

$$C^* = (3 \times 6^{3/2}\, \Phi)/4\pi\, N_A[\eta], \qquad (8)$$

where N_A is Avogadro's number, Φ is Flory–Fox constant $= 2.1 \times 10^{23}$ and $[\eta]$ is the intrinsic viscosity. Substitution of these values gives $C^* \approx 20$ g/l for gelatin. Several experimental techniques are used to study polymer gels. These can be classified into two categories: static and dynamic methods. The physical architecture is probed through static light scattering (SLS) and small angle X-ray and neutron scattering (SAXS and SANS), whereas dynamics is explored through dynamic light scattering (DLS), rheology, dielectric relaxation (DE) studies and fluorescence recovery after photobleaching (FRAP) methods. Here we shall confine our discussion to probing the gel state by laser light scattering (SLS and DLS). In this method, the system has refractive index n and is physically *seen* over a length scale q^{-1} where $q = (4\pi n/\lambda)\, \sin\theta/2$. The laser wavelength in the scattering medium is λ/n and θ is the scattering angle. Typically, q^{-1} is 50 nm and can be varied by a small amount by changing the scattering angle.

The normalized intensity auto-correlation function $g_2(q, t)$ measured by the digital correlator can be related to the dynamic structure factor $S(q, t)$ through the general expression[4–6]

$$g_2(q, t) = 1 + \beta\, [2X(1-X)\, S(q, t) + X^2\, |S(q, t)|^2], \qquad (9)$$

where β is the coherence area factor having maximum value $\beta = 1$. In a real experiment it defines the signal modulation which is a measure of signal-to-noise ratio of the data. The parameter X $(0 \le X \le 1)$ defines the extent of heterodyne contribution present in the measured $g_2(q, t)$ data. In the sol state $X = 1$ and the Siegert relationship $g_2(q, t) = 1 + |S(q, t)|^2$ gets established. However, in the gel state $X < 1$ and the term $2X(1-X)$ makes a finite contribution to $g_2(q, t)$ and hence it must be accounted for. The value of parameter X can be determined experimentally. The intercept of the plot of $[g_2(q, t)-1]$ versus delay time t at $t \to 0$ gives $\beta\, [2X-X^2]$ from which the value of X can be calculated if β is known. The estimation of $\beta < 1$ which is an instrumental factor, can be done easily by performing an experiment at a high temperature where the system, being in the sol state, shows zero heterodyne contribution. In Figure 3, variation of X with temperature has been shown explicitly for one of our samples. In the sol phase, we measured $X \approx 0.9$. Hence, $S(q, t)$ could be determined from $g_2(q, t)$ data directly, using Siegert relation. In the gel phase, $X \approx 0.1$, the prefactor of $S(q, t)$ term in eq. (9) is almost 20 times larger than the prefactor of $|S(q, t)|^2$. Thus we could neglect the contribution of the second term and fit the data to evaluate the various relaxation modes explicitly. The $g_2(q, t)$ data did not yield any fitting to a three mode relaxation model (triple exponential fitting) and neither to a single exponential relaxation model. The best fit could be established where $S(q, t)$ was assigned a form

$$S(q, t) = S_f(q, t) + S_s(q, t), \qquad (10)$$

where $S_f(q, t) = a\, \exp(-\Gamma_f t)$ and $S_s(q, t) = b\, \exp(-(\Gamma_s t)^{\alpha})$. In the sol state $S(q, t)$ data points were evaluated from

$$S(q, t) = [(g_2(q, t)-1)/\beta]^{0.5}, \qquad (11)$$

and in the gel state from

$$S(q, t) = [g_2(q, t)-1]/[2\beta X(1-X)]. \qquad (12)$$

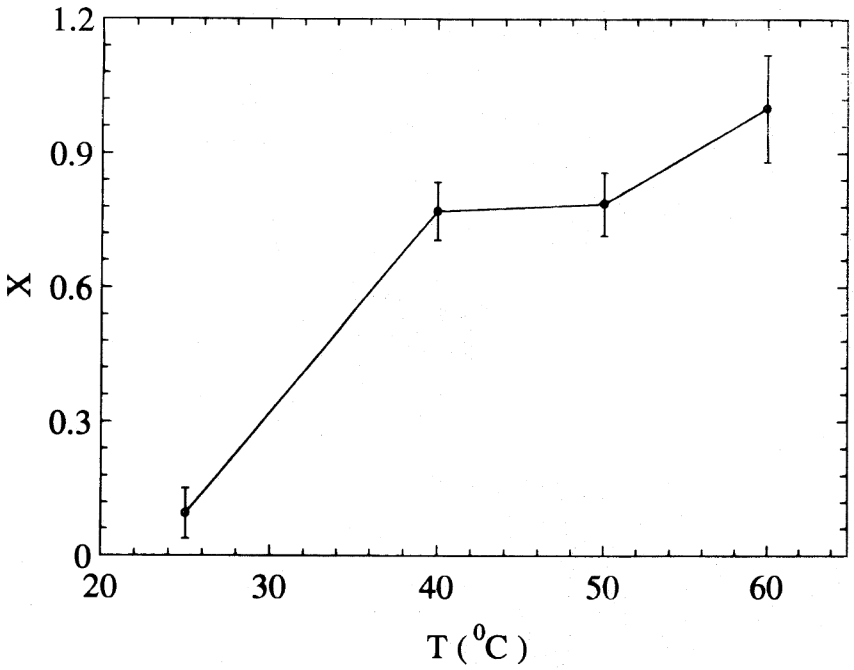

Figure 3. As the gel phase is approached, the initial total homodyne scattering process evolves to a heterodyne process as shown here. Here X is the heterodyne contribution to the scattered intensity signal. The gelation temperature of this system was 28°C.

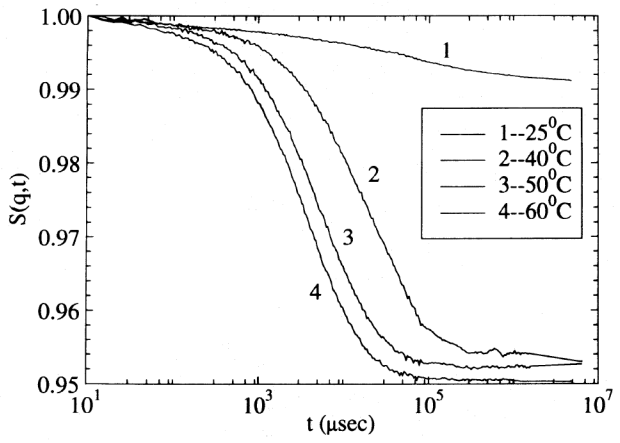

Figure 4. Evolution of the dynamic structure factor $S(q, t)$ with temperature T (shown in the inset). Sample was glutaraldehyde (GA) (0.001% w/v) crosslinked gelatin (5% w/v) in phosphate buffer (0.1 M) at pH = 6.8. See text for details.

The evolution of $S(q, t)$ as the gel phase was approached could be observed from Figure 4. The correlation data were split into two portions. For $t < 500$ μs, the correlation data were fitted to $S_f(q, t)$ and for $t > 500$ μs, the correlation data were fitted to $S_s(q, t)$.

Fast-mode relaxation

The diffusion coefficient of the fast mode was deduced from $D_f = \Gamma_f/q^2$. It is diffusive in nature. The fast mode diffusion is normally identified as the co-operative diffusion, D_c or the gel mode diffusion of the polymer network. The mesh size of the network can be deduced by balancing all forces acting on a blob (eq. (4)). The cooperative diffusion coefficient is related to the osmotic compression (K_{os}) and shear modulii (G_{os}) through the frictional coefficient of the blob per unit volume f, as[13]

$$D_c = E_{os}/f = (K_{os} + (4/3)\, G_{os})/f. \quad (13)$$

At equilibrium, the elastic energy associated with the network exactly counterbalances the combined thermal and osmotic energy that tend to disrupt the network. Any mismatch between these balancing forces can either lead to swelling or shrinking (dehydration) of the network. Eq. (13) leads to other interesting conclusions pertaining to the concentration dependence. For a system with no excluded volume interaction, K_{os} is determined by three body-interactions and thus

$$K_{os} \propto C^3. \quad (14)$$

On the other hand, the shear modulus is proportional to the probability of two polymer strands coming into contact. Hence $G \propto C^2$. The frictional coefficient f scales with concentration as $f \propto C^2$. This immediately leads to the conclusion that D_c is directly proportional to C. This can be generalized as follows[21].

$$D_c \propto C^{\gamma}, \tag{15}$$

where $\gamma = 0.77$ for good and 1.0 for theta (ideal situation where there is no excluded volume interaction) solvents. The gel network is associated with a characteristic renewal time or the lifetime of the network. As has already been mentioned, the gel network is in dynamic equilibrium where the mesh is constantly disturbed and restored over a characteristic time scale τ_r. This is related to the polymer concentration as[13,22]

$$\tau_r = A(C/C^*)^{\delta}, \tag{16}$$

with $A = (6\pi\eta/k_BT)R_g^3$, where the polymer has a radius of gyration of R_g. The exponent $\delta = 1.5$ for good solvents and 3.0 for theta solutions. These relations are derived for chemically cross-linked networks and gels. Some physical gels can exhibit significantly different exponents.

Since D_c is a measure of the rate of relaxation of local concentration gradients, it can be attributed to the cooperative movement of entangled transient networks of polymer chains. It has been argued earlier that as the temperature is reduced, the number of cross-linked chains increase. This would make ξ decrease with temperature as observed in our studies (Figure 5). There has been evidence of D_c showing just the opposite behaviour in sol phase. The increase in the concentration of cross-linked chains was observed to reduce the D_c values in sol phase. In the gel phase D_c showed no dependence on the concentration of cross-linked chains. Our results are contrary to these observations[5]. We attribute this discrepancy to the fact that early workers did not account for the heterodyne contribution to the $g_2(q, t)$ and hence the reported D_c values were not representative of fast mode relaxation. This was the case in most of the earlier studies. The rheological studies quantitatively bind to the fast mode diffusivity through the elastic modulii parameters.

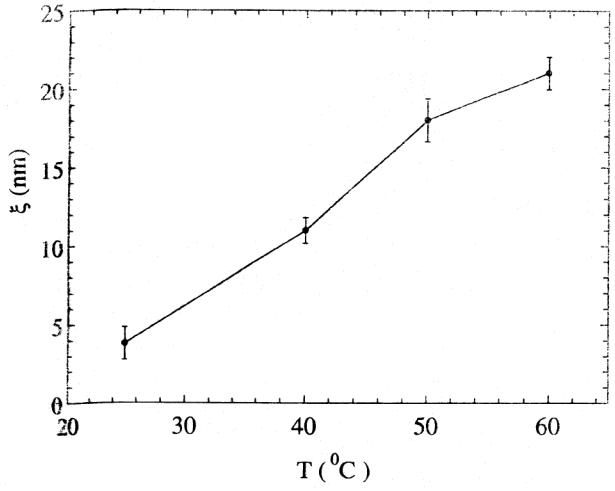

Figure 5. Average mesh size ξ of the cross-linked network as a function of temperature. The solid line is a guide to eye.

Slow-mode relaxation

The exact origin of the slow mode relaxation is still unresolved. The existence of slow mode in the sol phase has been pointed out by Borsali *et al.*[23], Amis *et al.*[24] and Herning *et al.*[15] among others. Amis *et al.* and Herning *et al.* attributed the presence of this slowly relaxing mode to the self-diffusion of a few polymer clusters through the rest of the solution. Such a description would be incompatible in a chemically cross-linked gel phase. For gelatin gels the slow mode component of the dynamic structure factor $S_s(q, t)$ was observed for 500 μs $< t <$ 1 s. The width of the relaxation time distribution function is given by α (see eq. (10)) which shows strong temperature dependence and no dependence on the concentration of the cross-linker GA. Pure gelatin solutions yield $\alpha = 0.75$ in the semi-dilute concentration regime. For gelatin–SDS complexes, α was measured to be 0.85 ± 0.09 in both sol and gel states of this polypeptide. Ren and Sorensen[25] showed that for pure gelatin α had a value 0.81 for the sol state and 0.67 for the gel state. Martin *et al.*[26], measured $\alpha = 0.65$ in gelling silica which is a chemically cross-linked gel. The glutaraldehyde cross-linked gelatin system studied here conforms to these data quite well at $T = 25°C$ and $T = 40°C$. Ren and Sorensen[25] observed a sharp transition in the α versus temperature plot at the gelation temperature. Cho and Sakasita[27] observed the slow mode relaxation frequency showing a sharp discontinuity at the gelation temperature. As has already been said earlier, these works did not account for heterodyning of the signal in the gel phase, thus their results for D_s would invariably contain a finite amount of error. Borsali *et al.*[23] fitted a stretched exponential function to $S_s(q, t)$ data and for the intermediate and concentrated gelatin solutions obtained an equivalent slow mode diffusivity D_s which scaled with gelatin concentration C as

$$D_s \approx C^{\sigma}, \tag{17}$$

with $\sigma = 1.31$, in the intermediate concentration regime and 2.73 in the concentrated regime, in close proximity to 1.2 and 2.75 measured by Amis *et al.*[24] for identical systems. In all these studies, the polypeptide chains were physically cross-linked as opposed to our case where both physical and chemical cross-links were present. A physical picture to this was given by Oikawa and Nakanishi[18]. Here the total cross-link density, was assumed as a sum of the chemical cross-linking density and physical cross-linking density. They calculated the

values of chemical cross-linking density assuming the chemical cross-link sites to be tetra functional. But, in their description of the slow mode dynamic structure factor, they used a single exponential decay, a formalism proved to be incorrect as we could not fit our data to a single exponential function and had to use a stretched exponential fitting for $S_s(q, t)$. We can define a slow mode diffusivity D_s as[28]

$$D_s = l^2/t_s = (t_s)^{\alpha-1} (\tau_c)^{-\alpha} q^{-2}, \quad (18)$$

from purely dimensional considerations. The slow mode relaxation time is τ_c. Realize that determination of D_s would necessitate *a priori* knowledge of t_s which is unknown. Presuming the center of mass diffusion of an imaginary particle of radius R, $D_s = k_B T/(6\pi\eta R)$. Here $\eta = \eta_{soln}$ will yield self-diffusion and $\eta = \eta_{solv}$ the center of mass motion in the solvent phase. It is well known that for a self-diffusion process $D_s \approx T/\eta_{soln}$ and for the diffusion of a solute in a solvent medium $D_s \approx T/\eta_{solv}$. Combining with eq. (18), a plot of $\ln(\eta_{soln}/T)$ versus $\ln\tau_c$ would yield a slope equal to α. Figure 6 shows a similar plot of and the average slope obtained was $\alpha = 1.3 \pm 0.2$ independent of GA concentration, in disagreement with the proposition of eq. (18). Despite these developments the origin of slowmodes remain unresolved.

Probe diffusion in gels

The diffusion of probe particles in a confined geometry has evoked considerable interest in the past because of its importance in providing basic understanding of transport of proteins through membranes in cells. In a solution phase the probe particle can explore the entire configurational space of the system and hence, the time averaged dynamic structure factor measured through dynamic light scattering (DLS) gives a good ensemble averaged picture of the whole system. There are situations, where because of geometrical constraints offered by the cross-linked networks of a gel, the probe particle gets confined and can execute only local excursions about its mean position. Thus it cannot explore the entire configurational space and the time averaged dynamic structure factor no longer is representative of the whole ensemble of the system. Here the data interpretation of DLS measurements becomes ambiguous. The non-Markovian Brownian motion of probe particles was investigated by Ohbayashi *et al.*[29]. The probe particles were used to measure micro-viscosity and channel size of sickle-cell haemoglobin gels by Madonia *et al.*[30] Allain *et al.*[31] studied the diffusion of probe particles in gelling copolymerization of acrylamide and bisacrylamide solutions and deduced the evolution of micro-

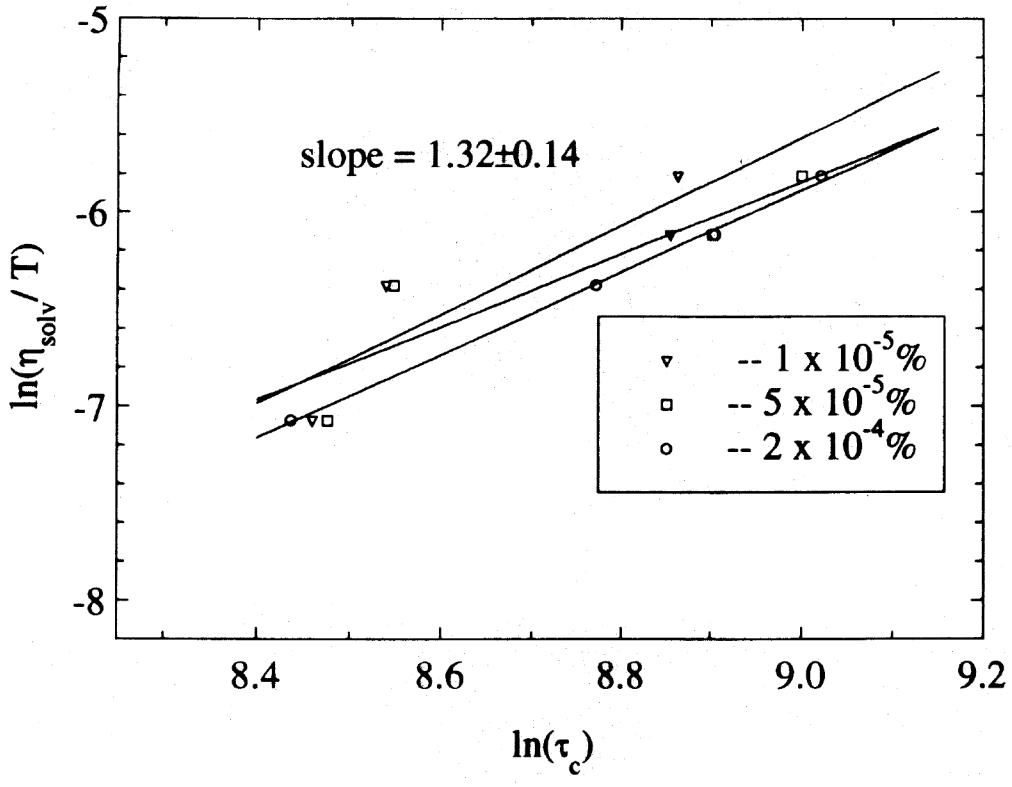

Figure 6. Plot of $\ln(\eta_{solv}/T)$ vs $\ln\tau_c$ for solutions with different concentrations of added GA in gelatin. The least-squares fit to a straight line gives average slope 1.3 ± 0.2 independent of GA concentration. See text for details.

viscosity. The wave vector q dependence of the probe diffusion was explored by Nishio *et al.*[32] in polyacrylamide gels and the pore size of the gel network where the cross-link content was varied through the gelation threshold was deduced from the DLS data. Djabourov *et al.*[33] adopted a similar approach and explored colloidal probe diffusion in a physical gel. Subsequently, Reina *et al.*[34] reported observation of a complex dynamical behaviour ranging from the purely translational diffusion of the probe particles in the medium to a relaxational behaviour associated with the local motion of probe particles in a confined space inside the gel. The dynamics of probe particles in a semi-dilute polymer solution was quantified through a set of phenomenological scaling laws by Phillies *et al.*[35] The molecular weight dependence of probe diffusion in polyacrylamide gels was studied in detail by Tokita *et al.*[36] Pusey and van Megen[37] proposed the ergodic to non-ergodic transition as seen by the probe particles during the sol to gel transition process through an elegant mathematical model which was almost overlooked until then. Subsequently, they could apply their model to a chemically cross-linked gel (polyacrylamide) and study the dynamics of probe particle diffusion in these gelling solutions. The effect of inhomogeneities in gels was explored by Suzuki and Nozaki[38] through DLS studies.

The purpose here was to study the evolution of dynamic structure factor of the light scattered from the probe particles in a gelling solution. The transport properties like diffusivity of the probe and microscopic viscosity 'seen' by the probe as the medium goes from an ergodic medium (solution phase, a system which on given enough time, evolves through all representative domains of all spatial configurations), to a gel state (a non-ergodic system where the spatial configurations explored do not span the whole configurational space), has been explored in detail. The essence of Pusey and Van Megen proposition can be summarized as follows and we have also performed an *ab initio* derivation of these results[39]. The assumptions made by us are the following: (1) time-averaged properties of a particular volume of a non-ergodic medium is equivalent to an average over a sub-ensemble of all the configurations achieved by restricted displacements of the scatterers about fixed positions. (2) The total field scattered by a particular volume is written as the sum of fluctuating (effectively ergodic) component and a constant (non-ergodic) component. (3) The diffusion coefficient D is q dependent and yields the gradient diffusion coefficient in $q \to 0$ limit.

The intensity correlation function (ICF) measured by DLS is defined as (called $g_2(q, t)$ earlier) a time-averaged function

$$ICF = \langle I(0)I(\tau)\rangle = \lim_{T\to\infty} (1/T) \int_0^T dt I(t)I(t+\tau). \quad (19)$$

In an ergodic medium, the scatterers are highly delocalized, hence on being given enough time any particular sub-ensemble of the system would evolve through all the spatial configurations of the system. Thus we can say that the time average of the intensity correlation function $\langle ICF\rangle_T$ and the ensemble averaged intensity correlation function $\langle ICF\rangle_E$ are equal.

As a consequence, the information obtained from studying the time-averaged intensity correlation function of a particular sub-ensemble of the system is applicable to the entire system. However, as the system moves towards non-ergodicity, the scatterers become more and more localized and suffer fluctuations about their mean positions only. Hence, by just studying the time-averaged intensity correlation function of a sub-ensemble of the system one does not get knowledge of the system as a whole. If one wants to study $\langle ICF\rangle_E$ of the system then a huge amount of experimental time and averaging over a lot of sub-ensembles of the system would be required.

Pusey and van Megen[37] showed that from a single shot DLS measurement performed on a non-ergodic medium, it was possible to extract the exact dynamic structure data. Let us recapitulate some of the useful relations that have been used in our studies[39]. The non-ergodicity parameter Y is defined as the ratio between ensemble and time-averaged intensity

$$Y = \langle I(q)\rangle_E / \langle I(q)\rangle_T, \quad (20)$$

and consequently, the normalized ICF, $g_2(q, t)$ can be written as

$$g_2(q, t)_T = Y^2 [S(q, t) - S(q, \infty)]^2 + 1. \quad (21)$$

Defining $\langle I^2(q)\rangle_T / \langle I(q)\rangle^2_T = \sigma_I$, it is possible to show that the dynamic structure factor $S(q, t)$ becomes

$$S(q, t) = [g_2(q, t)_T - 1]^{1/2} (1/Y) + (1-\sigma_I). \quad (22)$$

This will yield an effective diffusion coefficient D that will be a function of (Y, σ_I).

We dispersed a trace amount of polystyrene latex particles in a gelling solution of gelatin at 60°C. The latex particles had a nominal diameter of 90 nm (Fluka Scientific, USA) and the volume fraction of this in solution was about 5×10^{-5}. The differential scattering observed from the latex solution was more than 10 times the gelation solution. The solution was then kept in an ultrasonic vibrator for 30 min to homogeneously disperse the solutes. This was transferred into clean borosilicate glass cells and sealed. The sample was allowed to cool spontaneously to room temperature. Each measurement lasted for about 3 min (probe particles are very strong scatterers) over which the temperature fell by less than 0.5°C. To measure the ensemble averaged

intensity values, we rotated and translated the sample cell to choose as many scattering volumes as possible. The entire span of experiment lasted for more than 24 h. The ergodicity parameter Y was calculated using eq. (20) and is plotted as function of gelation time in Figure 7. For an ergodic medium Y was very well defined and was almost equal to 1, but after about 3 hours the onset of gelation took place and the medium was rendered non-ergodic. This made Y highly undefined (Figure 7) and started fluctuating about 1. In fact, Y takes a value depending upon the subensemble of the medium under study. One can associate this observation to the evolution of the non-ergodic nature of the medium. This has further bearing on the ICF measured by the digital correlator. When the medium is ergodic, the scatterers execute unrestricted Brownian motion and the intensity $I(q, t)$ of the speckle pattern will fluctuate with time. Furthermore, in time a representative fraction of all possible configurations of the scatterers will eventually be sampled so that in turn, the speckle pattern will undergo full range of Gaussian fluctuations. Hence for a perfectly ergodic state $g_2(q, 0)_T$ will have its maximum value. As the process of gelation onsets, the scatterers suffer only limited fluctuations about some fixed points and get localized. Now the probes do not evolve through all possible spatial configurations hence only a restricted range of fluctuations is sampled causing $g_2(q, 0)_T$ to steadily decrease with progress of gelation. This phenomenon can be clearly observed from Figure 8. The long time diffusion coefficient is a measure of the collective motion of both the medium and the probe particles. The long time diffusion coefficient gets lowered as one moves from a completely fluctuative medium to a medium where the bulk movement of the network and the solvent trapped in it takes place. It can thus be argued that the long-term diffusion coefficient is associated with the local viscosity of the medium through Stokes–Einstein relation.

$$\eta_l = k_B T/6\pi RD, \tag{23}$$

where η_l is the coefficient of local viscosity observed by the probe particle (microscopic viscosity), R is radius of the probe particle, k_B is Boltzmann constant, T is absolute temperature and D is long time diffusion coefficient. From Figure 9, it is observed that after gelation the coefficient of viscosity remains almost constant. The evolution of micro-viscosity can be effectively

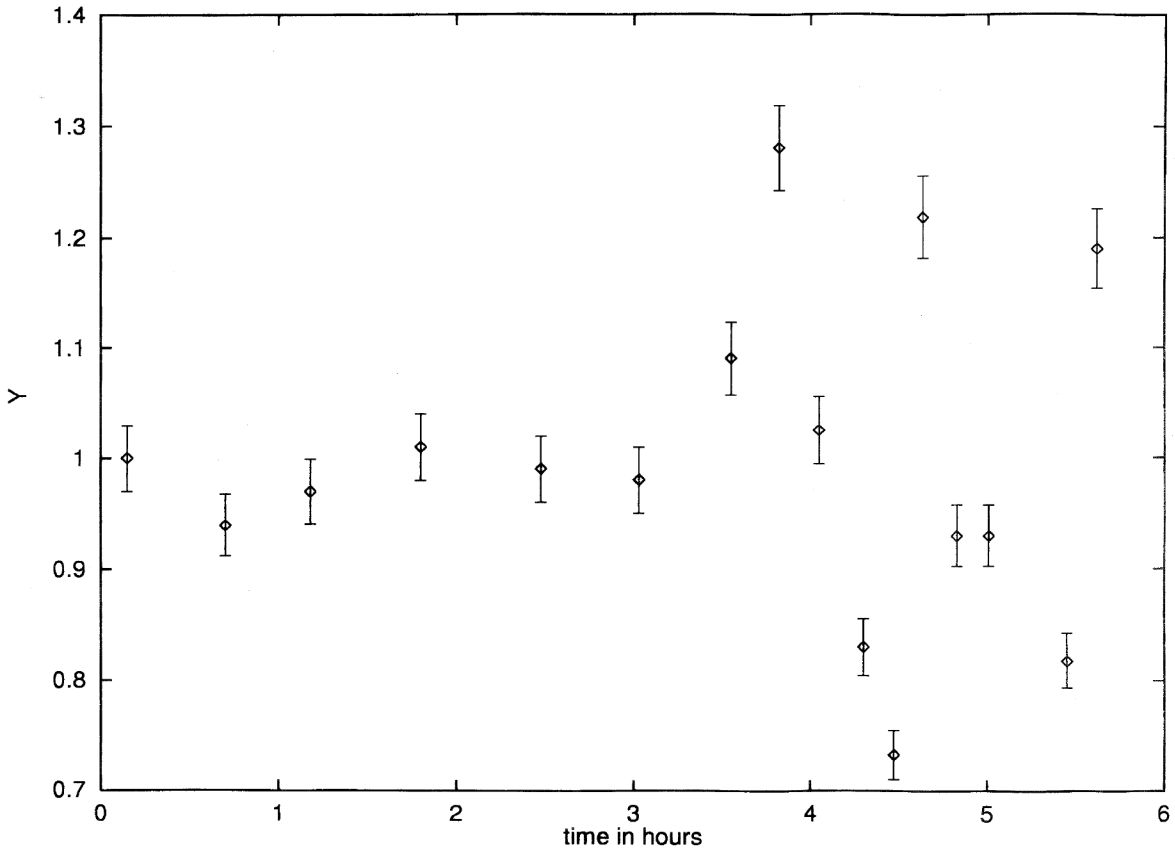

Figure 7. Evolution of the non-ergodicity parameter Y as a function of time. The hot sol sets into a soft gel in about 180 min. During this period Y is close to 1 implying the system was completely ergodic. After that a random Y value signifies loss of ergodicity for the medium.

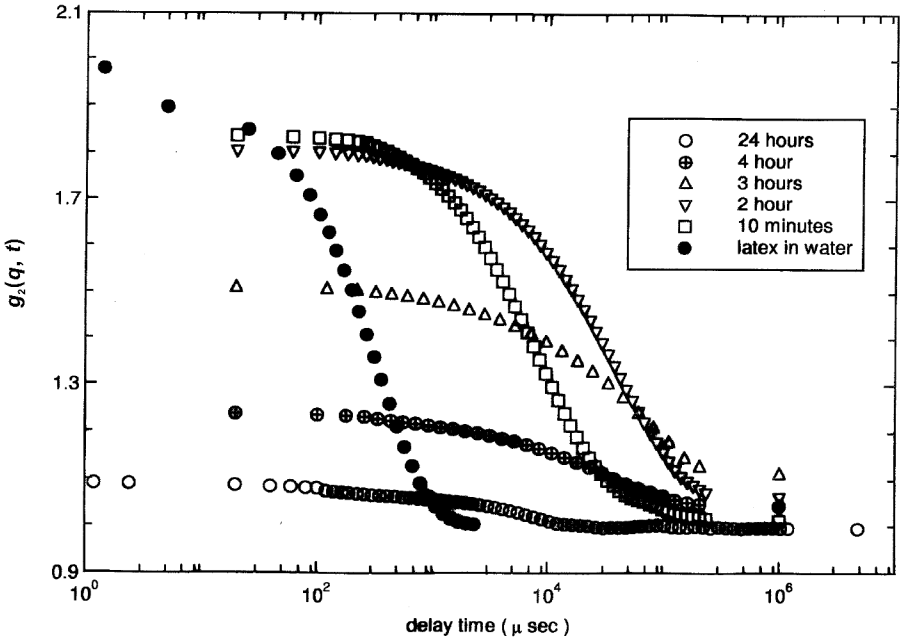

Figure 8. The same process as described in Figure 7. Here we show the evolution of the intensity correlation function $g_2(q, t)$ with time. A single exponential feature is seen for latex in water. For the gelling solution, $g_2(q, t)$ shows significantly different relaxation feature for time scales larger than 3 h (typically).

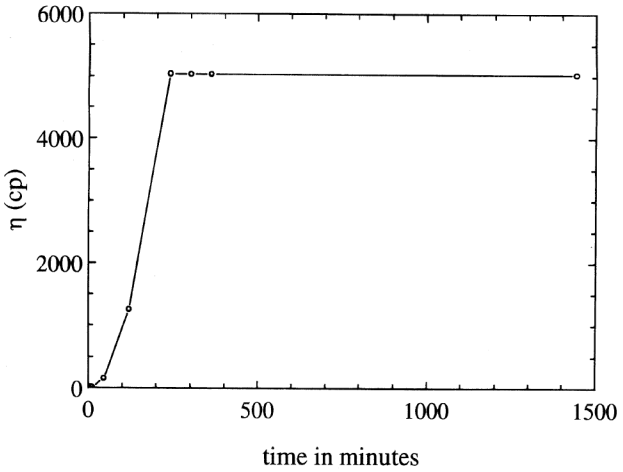

Figure 9. Growth of medium micro-viscosity η_l, as a function of temperature. The sol state has a viscosity of ~ 1 cP that grows to ~ 4500 cP once gel is formed. See text for details.

probed if we assume that there was no polymer adsorption on the surface of the latex particles. This allows us to use $R = 45$ nm and we could estimate the value of 'microscopic viscosity' (the viscosity of the region where the probe particle has been trapped) from eq. (23). The viscosity had a sol state value of almost 1 cP (at 60°C) which gradually increased to almost 5000 cP (at 20°C) as the onset of gelation takes place at time ≈ 180 min. Beyond this time the viscosity retained a plateau value. This high viscosity is responsible for arresting the center of mass motion of the latex spheres. In this calculation we neglect the effect of solvent adsorption on the latex surface.

Conclusion

The general feature seems to be that as the gelation point is approached, the fast mode relaxation time decreases and slow mode relaxation time increases continuously. The same feature is observed for their amplitudes. The slow mode amplitude and relaxation time peak at the gelation point. The slow mode relaxation time behaviour exactly follows[40] the trend of rheological relaxation time temperature dependence and both peak at T_{gel}.

It is worthwhile to make a statement about the solvent state that is trapped in the network structure. The solvent separates into two distinguishable states. Part of the solvent is free and the rest is inside the core as interstitial solvent. The interstitial water and the bulk water in the gel phase can have significantly different physical properties, and these can be distinctly seen by IR and Raman spectroscopy. The interstitial water comprises of hydration water and the water trapped inside the gel network[41].

Polymer gels and networks are a novel state of matter where the elasticity and fluidity can be tuned to one's requirement. In the next decade, synthetic polymers will be slowly replaced by bio-polymers because of environmental demands. Some of other applications being pursued are the following. A certain family of reverse

micelles contain large pools of water in their cores. These pools have a radius of several nanometers and can be used as micro-reactors for carrying out chemical reactions. These can also be used to host polymers, proteins, enzymes, etc. Once this is achieved, these can be used as carriers of drug to the target. The problem involves systematic study of this encapsulation behavior, bio-activity of trapped polymers and its over-all characterization and optimization. It will be challenging to see if a cross-linked network or a gel could be created inside these cores. Again a variety of experimental techniques will be needed to probe and understand such a system. A wide variety of bio-polymers form physical networks which often culminates in gelation. Efforts are on to grow living cells using the networks as scaffoldings; maybe one day this will lead to cultivation of customer-designed organs. Here again, the objective will be to study their rheological behaviour to understand the salient features and dynamics of these structures. A clear understanding of network structure is essential for any future application. Considering the application potential of these systems, it will be worthwhile for scientists drawn from many different fields to join hands and work together.

1. Herman, P. H., in *Colloid Science-II* (ed. Kruyt, H. R.), Elsevier, Amsterdam, 1949, pp. 483–504.
2. Ferry, J. D., *Visco-elastic Properties of Polymers*, John-Wiley, New York, 1980, pp. 529–540.
3. Almdal, K., Dyre, J., Hvidt, S. and Kramer, O., *Poly. Gels Networks*, 1993, **1**, 5 –12.
4. See for example *Thermoreversible Networks: Advances in Polymer Science* (ed. Nijenhuis, K. Te.), 1997, **130**, 1–7.
5. Bohidar, H. B. and Jena, S. S., *J. Chem. Phys.*, 1993, **98**, 3568–3570 and 8970–8977; *ibid*, 1994, **100**, 6888–6895; Sharma, J. and Bohidar, H. B., *Europ. Polym. J.*, 2000, **36**, 1409–1418 and *ibid*, *Colloid and Polym. Sci.*, 2000, **278**, 15–21.
6. See for example *The Wiley Polymer Network Group Review Series* (eds Nijenhuis, K. Te. and Mijs, W. J.), John Wiley and Sons, UK, 1998, vol. I.
7. Dietler, G. and Cannel, D. S., *Phys. Rev. Lett.*, 1988, **60**, 1852–1860.
8. Corti, M., Minero, M. and Degiorgio, V., *J. Phys. Chem.*, 1984, **88**, 309–405.
9. Li, Y. and Tanaka, T., *J. Chem. Phys.*, 1989, **90**, 5161–5170.
10. Flory, P. J., *Principles of Polymer Chemistry*, Cornell University Press, Ithaca, 1953.
11. Morton, S. D. and Ferry, J. D., *J. Phys. Chem.*, 1962, **66**, 1639–1648.
12. Tanaka, T., in *ACS Symposium Series–480* (eds Harland, R. S. and Prud'homme, R. K.), 1990, pp. 1–3.
13. de Gennes, P. G., *Scaling Concepts in Polymer Physics*, Cornell University Press, Ithaca, New York, 1979.
14. Djabourov, M., *Contemp. Phys.*, 1988, **29**, 273–297.
15. Herning, T., Djabourov, M., Leblond, J. and Takekart, G., *Polymer*, 1991, **32**, 3211–3218.
16. Busnel, J. P. and Ross-Murphy, S. B., *Int. J. Biol. Macromol.*, 1989, **11**, 119–125 and 1988, **10**, 121–125.
17. Godard, P., Biebuyck, J. J., Daumerie, M., Naveau, H. and Mercier, J. P., *J. Polym. Sci., Polym. Phys.*, 1978, **16**, 1817–1825.
18. Oikawa, H. and Nakanishi, H., *Polymer*, 1993, **34**, 3358–3364.
19. Wards, A. G. and Courts, A., *The Science and Technology of Gelatin,* Academic Press, London, 1977.
20. Doi, M. and Edwards, S. F., *The Theory of Polymer Dynamics*, Harper and Row, Clarendon Press, Oxford, 1986.
21. Yamakawa, H., *Modern Theory of Polymer Solutions*, Harper and Row, New York, 1971.
22. Doi, M., *Introduction to Polymer Physics*, Oxford Science Publications, Oxford, 1995.
23. Borsali, R., Durand, D., Fisher, E. W., Geibel, L. and Busnel, J. P., *Polym. Networks Blends*, 1991, **1**, 11–26.
24. Amis, E. J., Janmey, P. A., Ferry, J. D. and Yu, H., *Macromol.*, 1983, **16**, 441–451.
25. Ren, S. Z. and Sorensen, C. M., *Phys. Rev. Lett.*, 1993, **70**, 1727–1730.
26. Martin, J. E., Wilcoxon, J. and Odinek, J., *Phys. Rev.*, 1991, **A43**, 858–872.
27. Cho, M. and Sakasita, H., *J. Phys. Soc. Jpn.*, 1996, **65**, 2790–2792.
28. Maity, S. and Bohidar, H. B., *Phys. Rev.*, 1998, **E58**, 729–737.
29. Ohbayashi, K., Kohno, T. and Utiyama, H., *Phys. Rev.*, 1983, **A27**, 2632–2641.
30. Madonia, F., San Biagio, P. L., Palma, M. U., Schiliro, G., Musumeci, S. and Russo, G., *Nature*, 1983, **302**, 412–415.
31. Allain, C., Drifford, M. and Gauthier-Manuel, B., *Polym. Commun.*, 1986, **27**, 177–180.
32. Nishio, I., Reina, J. C. and Bansil, R., *Phys. Rev. Lett.*, 1987, **59**, 684–687.
33. Djabourov, M., Grillon, Y. and Leblond, J., *Polymer Gels Networks*, 1995, **3**, 407–428.
34. Reina, J. C., Bansil, R. and Konak, C., *Polymer*, 1990, **31**, 1038–1044.
35. Phillies, G. D. J., Ullmann, G. S., Ullmann, K. and Lin, T. H., *J. Chem. Phys.*, 1985, **82**, 5242–5246.
36. Tokita, M., Miyoshi, T., Takegoshi, K. and Hikichi, K., *Phys. Rev. Lett.*, 1996, **53**, 1823–1827.
37. Pusey, P. N. and van Megen, W., *Physica A*, 1989, **157**, 705–741.
38. Suzuki, Y. and Nozaki, K., *J. Chem. Phys.*, 1992, **97**, 3808–3812.
39. Ghosh, S., M S thesis, School of Physical Sciences, Jawaharlal Nehru University, New Delhi, 1999; limited copies are available on request. See also Bohidar, H. B. and Ghosh, S., *Eur. Polym. J.*, 2000, in press.
40. Burchard, W., Aberle, T. H., Fuchus, T., Richtering, W., Coviello, T. and Geissler, E., in *Chemical and Physical Networks* (eds Nijenhuis, K. Te. and Mijs, W. J.), John Wiley & Sons, New York, 1998, p. 13–23.
41. Maity, S., Jena, S. S., Pradhan, A. and Bohidar, H. B., *Colloid Polym. Sci.*, 1999, **277**, 666–672.

ACKNOWLEDGEMENTS. Most of the experimental results cited here have originated from the research work of my students namely, Jitendra Sharma and Shankar Ghosh. This was written when I was on sabbatical leave from School of Physical Sciences, Jawaharlal Nehru University, New Delhi. The hospitality extended by the faculty and staff of Chemistry Department of Purdue School of Science at Indianapolis, USA is gratefully acknowledged.